



Instantaneous Achievement of the Hall and Pedersen–Cowling Current Circuits in Northern and Southern Hemispheres During the Geomagnetic Sudden Commencement on 12 May 2021

Takashi Kikuchi^{1*}, Tohru Araki², Kumiko K. Hashimoto³, Yusuke Ebihara⁴, Takashi Tanaka⁵, Yukitoshi Nishimura⁶, Geeta Vichare⁷, Ashwini K. Sinha⁸, Jaroslav Chum⁹, Keisuke Hosokawa¹⁰, Ichiro Tomizawa¹¹, Yoshimasa Tanaka^{12,13,14} and Akira Kadokura^{12,13,14}

OPEN ACCESS

Edited by:

David Gary Sibeck,
National Aeronautics and Space
Administration, United States

Reviewed by:

Arnaud Masson,
European Space Astronomy Centre
(ESAC), Spain
Octav Marghitu,
Space Science Institute (Romania),
Romania

*Correspondence:

Takashi Kikuchi
kikuchi@isee.nagoya-u.ac.jp

Specialty section:

This article was submitted to
Space Physics,
a section of the journal
Frontiers in Astronomy and Space
Sciences

Received: 19 February 2022

Accepted: 12 April 2022

Published: 31 May 2022

Citation:

Kikuchi T, Araki T, Hashimoto KK, Ebihara Y, Tanaka T, Nishimura Y, Vichare G, Sinha AK, Chum J, Hosokawa K, Tomizawa I, Tanaka Y and Kadokura A (2022) Instantaneous Achievement of the Hall and Pedersen–Cowling Current Circuits in Northern and Southern Hemispheres During the Geomagnetic Sudden Commencement on 12 May 2021. *Front. Astron. Space Sci.* 9:879314. doi: 10.3389/fspas.2022.879314

¹Institute for Space–Earth Environmental Research, Nagoya University, Nagoya, Japan, ²Geophysical Institute, Kyoto University, Kyoto, Japan, ³School of Agriculture, Kibi International University, Minamiawaji, Japan, ⁴Research Institute for Sustainable Humanosphere, Kyoto University, Kyoto, Japan, ⁵International Center for Space Weather Science and Education, Kyushu University, Fukuoka, Japan, ⁶Research Associate Professor, Center for Space Physics, Boston University, Boston, MA, United States, ⁷Indian Institute of Geomagnetism, New Mumbai, India, ⁸Department of Physics, University of Bahrain, Bahrain, India, ⁹Department of the Ionosphere and Aeronomy, Institute of Atmospheric Physics of the Czech Academy of Sciences, Prague, Czechia, ¹⁰Department of Communication Engineering and Informatics, University of Electro-Communications, Chofu, Japan, ¹¹Center for Space Science and Radio Engineering, The University of Electro-Communications, Chofu, Japan, ¹²National Institute of Polar Research, Tachikawa, Japan, ¹³Research Organization of Information and Systems, Joint Support-Center for Data Science Research, Polar Environment Data Science Center, Tachikawa, Japan, ¹⁴The Graduate University for Advanced Studies, SOKENDAI, Tachikawa, Japan

The present article aims at a consistent understanding of observation, theoretical model, and simulation with the geomagnetic sudden commencement (SC) observed in the morning and afternoon at high and middle latitudes in the northern and southern hemispheres and at the noontime equator on 12 May 2021. The SC in B_x - and B_y -components of the geomagnetic field, $SC_{x,y}$, was composed of the positive/negative preliminary (PI) and main impulses (MI) as SC_x (+ -) and SC_y (- +) in the morning and SC_x (- +) and SC_y (+ -) in the afternoon at middle latitudes in the northern hemisphere. SC_x in the southern hemisphere is in the same polarity as those in the northern hemisphere, except for SC_x (+ +) in the morning. SC_y in the southern hemisphere has reverse polarity to those in the northern hemisphere. The Pl_x in the northern hemisphere matches the well-established two-cell Hall current vortices with anti-clockwise and clockwise directions in the morning and afternoon, respectively, and the Ml_x matches reverse Hall current vortices. The Pl_x and Ml_x in the southern hemisphere meet the Hall currents that are mirror images of those in the northern hemisphere with respect to the equator except for the

Abbreviations: DL, stepwise low latitude magnetic disturbance; EEJ, equatorial electrojet; GML, geomagnetic latitude; HF, high frequency; MFD, main frequency deviation; MHD, magnetohydrodynamic; MI, main impulse; MLT, magnetic local time; PFD, preliminary frequency deviation; PI, preliminary impulse; SC, geomagnetic sudden commencement; SCF, SC-associated Doppler frequency; TM_0 , zeroth-order transverse magnetic.

positive MI in the morning. The Ply in the northern hemisphere is shown to meet the northward and southward Pedersen currents in the morning and afternoon, respectively, and the Mly meets reverse Pedersen currents. The Ply and Mly in the southern hemisphere are found to meet the Pedersen currents that are mirror images of those in the northern hemisphere. At the equator, typical SCx (- +) is observed, meeting the Cowling currents that should be supplied by the Pedersen currents responsible for the observed midlatitude SCy in the northern and southern hemispheres. The electric fields of the PI and MI observed by the HF Doppler sounders at the middle latitudes in the northern hemisphere are westward and eastward, respectively, in both the morning and afternoon, meeting the conventional dusk-to-dawn PI and dawn-to-dusk MI electric fields. The onset of the PI is found to be simultaneous with the resolution of a few seconds from high latitude to the equator in both the northern and southern hemispheres, indicating instantaneous achievement of the Pedersen–Cowling currents from high latitude to the equator. The instantaneous achievement of the energy-consuming Pedersen–Cowling currents is explained by the TM_0 /TEM mode wave in the Earth-ionosphere waveguide/transmission line rather than the compressional waves in the magnetosphere and F-region ionosphere. REPPU (REProduce Plasma Universe) global simulation model equipped with a potential solver at the inner boundary of the model magnetosphere reproduces the PI and MI electric fields at middle latitudes and SCx (- +) at the dayside equator. The simulation results are found to be consistent with most features of observations, such as the time scale of PI and MI, direction of the midlatitude electric field and generation of the Cowling currents. The simulation proves that the electric fields and FACs are generated in the outer magnetosphere, transmitted to the polar ionosphere and then to the equator in the Pedersen–Cowling current circuit.

Keywords: geomagnetic sudden commencement, Hall current circuit, Pedersen–Cowling current circuit, simultaneous onset of preliminary impulse, morning/afternoon symmetry/asymmetry, northern and southern hemispheric symmetry/asymmetry, HF Doppler sounder, global simulation

INTRODUCTION

The geomagnetic sudden commencement (SC) caused by the solar wind shock/discontinuity is composed of a step-like magnetic increase (DL: disturbance at low latitude), preliminary impulse (PI) and main impulse (MI) (Araki, 1994 and references therein). The SC represents a change in B_x -component of the magnetic field in most cases. In the present article, we use SC_{x,y}, PI_{x,y} and MI_{x,y} to represent those in B_x - and B_y -components, while DL is used as is. The time scales of PI_x and MI_x are 1 min and 5–10 min, respectively. The DL is caused by the magnetopause currents, and the PI_x and MI_x are caused by the ionospheric Hall current vortices driven by the dusk-to-dawn and dawn-to-dusk electric fields, respectively. The PI_x currents are in counter-clockwise and clockwise directions in the morning and afternoon, respectively and therefore, the PI_x is positive (PPI: Preliminary positive impulse) and negative (PRI: preliminary reverse impulse) in the morning and afternoon, respectively at high and middle latitudes. The MI_x currents are in reverse direction to those of the PI_x. The two-cell Hall current vortices are estimated from the global magnetometer networks as the equivalent ionospheric currents (Vichare et al., 2014; Kikuchi et al., 2016). Thus, the type of SCx is SCx (+ -) in the

morning and SCx (- +) in the afternoon. The SCx is in phase in the northern and southern hemispheres with greater amplitude in summer hemisphere, because the MI_x currents flow in the ionosphere with higher conductivity in summer (Yumoto et al., 1996). The PI_x and MI_x electric field and currents are supplied with field-aligned currents (FACs) generated by dynamos in the outer magnetosphere (Slinker et al., 1999; Fujita et al., 2003a; Fujita et al., 2003b). Therefore, the polarity of the PI_x changes from positive/negative to negative/positive as one moves to higher latitude across the foot of the upward/downward FACs (Kikuchi et al., 2016).

The SCx at the dayside equator is enhanced with the latitudinal and longitudinal profiles of amplitude similar to those of diurnal variations (Rastogi, 1993; Rastogi et al., 2001) and with amplitude peaks before noon (Nilam et al., 2020). The equatorial enhancement of SCx is caused by the Cowling currents, i.e., Pedersen currents intensified by the Cowling effects (Hirono, 1952; Baker and Martyn, 1953). As a result, the equatorial SCx on the dayside is SCx (- +) composed of the DL superimposed by the negative PI_x and positive MI_x. The Cowling currents in the night are weak, but the night SCx begins with a two-step increase due to a small PPI (Araki et al., 1985). The nighttime DL is superimposed by magnetic field caused by the

Region-1 type FACs of the MI, which results in larger amplitude in the night than in the day and larger amplitude at higher latitudes around the midnight (Araki et al., 2006; Shinbori et al., 2009).

The SC in the Y-component of the geomagnetic field (SC_y) is caused by the Pedersen currents at middle latitude, so the Mly is positive/negative in the morning/afternoon (Tsunomura, 1998). The midlatitude Pedersen currents are supposed to achieve a current circuit from FACs at high latitude to the Cowling current at the equator (Kikuchi and Araki, 1979).

The electric fields of the PI and MI cause ionospheric plasma motion at middle latitudes as observed by the HF Doppler sounders with temporal resolution of 10 s (Kikuchi et al., 1985; Sastri, 2002; Kikuchi et al., 2016; Kikuchi et al., 2021). The SC-associated HF Doppler frequency deviations (SCF) are mostly in a bipolar structure as SCF (+ -) and SCF (- +) composed of the preliminary (PFD) and main (MFD) frequency deviations (Huang et al., 1973; Kikuchi et al., 1985). Kikuchi et al. (1985) showed that SCF (+ -) appears in the day and evening, and SCF (- +) in the night. The day-night reversal of PFD and MFD are caused by the dusk-to-dawn and dawn-to-dusk electric fields, respectively. The evening anomaly of the electric fields is due to the dawn-dusk asymmetry in the distribution of electric potential transmitted from the polar ionosphere (Tsunomura, 1999).

The onset of the PI_x was found to be simultaneous within the temporal resolution of 10 s at all latitudes (Araki, 1977), and the onset of the PFD observed at middle latitudes has been shown to be simultaneous with the PI_x at high and equatorial latitudes on the day- and night-sides (Kikuchi et al., 2021). Araki (1977) showed that the onset of the PI_x is earlier than the DL by several 10 s of sec, probably because of difference in the propagation time between along and perpendicular to the magnetic field lines as deduced from earlier onset of the PFD than DL at middle latitude (Kikuchi, 1986). The PI currents are transmitted from the magnetopause dynamo down the magnetic field lines *via* FACs (Tamao, 1964a; Tamao, 1964b; Slinker et al., 1999; Fujita et al., 2003a), while it takes some more time for the DL to propagate in the equatorial plane of the magnetosphere and plasmasphere *via* the fast (compressional) mode wave (Chi et al., 2006). In extreme solar wind conditions, however, the DL can arrive earlier than the PI_x currents as observed during the SC on 29 October 2003 (Kikuchi et al., 2016). In this extreme event, no PI_x appears at the equator because of overwhelming DL, but PI appears in the equatorial Cowling currents and PFD at midlatitude, because both PFD and Cowling current are not associated with DL, but associated with the PI current from the polar to equatorial ionosphere.

As overviewed above, ground magnetometer and HF Doppler sounder observations have shown that the electric field and currents are transmitted from the polar ionosphere to the equator near-instantaneously. Wave modes that allow rapid propagation have been studied using the compressional waves in the magnetosphere and/or in the F-region ionosphere (Tamao, 1964a; Tamao, 1964b; Chi et al., 2006; Lysak et al., 2015; Tu and Song, 2019) or using the TM₀/TEM mode waves in the Earth-ionosphere waveguide/transmission line (Kikuchi et al., 1978; Kikuchi and Araki, 1979; Kikuchi, 2014). The Alfvén speed of the

compressional waves can be applied to near-instantaneous propagation, and the Hall currents responsible for the PI_x may be explained by the mode conversion from the compressional waves (Tamao, 1964a; Tamao, 1964b; Lysak et al., 2015). However, we need to explain the overall characteristics of the electric field, including the day-night reversal (Kikuchi et al., 2021) and evening anomaly with the same direction as in the day (Kikuchi et al., 2016). Furthermore, we should explain the instantaneous achievement of the polar to equatorial ionospheric currents and energy consumption in the midlatitude Pedersen and equatorial Cowling currents. The Pedersen/Cowling currents have never been explained by means of the compressional waves. Kikuchi et al. (2016) showed that the midlatitude F-region ionosphere is not compressed by the compressional waves, which indicates no contribution of the compressional waves on the energy input to the midlatitude ionosphere. Kikuchi (2014) showed that the TM₀/TEM mode waves transmit the ionospheric electric potential and Pedersen currents to the equator, achieving the Pedersen–Cowling current circuit near-instantaneously. The present article aims at consistent understanding of observations of ionospheric electric fields and ground magnetic fields, waveguide/transmission line model, and global simulations by analyzing the SC event that occurred on 12 May 2021. For this purpose, we examine local time and latitudinal characteristics of the SC_x and SC_y observed in the northern and southern hemispheres, electric fields observed by HF Doppler sounders at middle latitudes in the northern hemisphere and reproduction of the midlatitude electric fields and equatorial SC_x by the global simulation. In particular, SC_y is focused on from the viewpoint of the Pedersen–Cowling current circuit as an energy channel from the polar to the equatorial ionosphere. We use magnetometer data from the northern and southern hemispheres in the morning and afternoon and from the equator at noon, and the HF Doppler sounder data from Czechia and Japan in the morning and afternoon, respectively. As shown below, the morning/afternoon and northern/southern hemispheric symmetry/asymmetry of SC_x and SC_y are consistent with the Hall and Pedersen–Cowling current circuits that are mirror images of each other in the northern and southern hemispheres. Furthermore, the onset of the PI_y is found to be simultaneous over the globe within a few seconds even when PI_x begins with delays of tens of seconds. The simultaneous onset proves the instantaneous achievement of the global Hall and Pedersen–Cowling current circuits by the TM₀/TEM mode waves propagating at the speed of light in the Earth-ionosphere waveguide/transmission line (Kikuchi et al., 1978; Kikuchi and Araki, 1979; Kikuchi, 2014). The HF Doppler sounders operated in the morning (Czechia) and afternoon (Japan) help ensure that the PI and MI electric fields are typical from dusk-to-dawn and dawn-to-dusk, respectively. We discuss that the SC electric fields are potential fields associated with ionospheric currents flowing from the polar to equatorial ionosphere by reproducing midlatitude electric fields and Cowling currents with the REPPU global simulation model. The REPPU model employs the potential solver that solves the current continuity equation with the FACs as an input at the inner boundary of the model

TABLE 1 | List of the magnetometer stations of INTERMAGNET, Indian Institute of Geomagnetism (IIG), and National Institute of Polar Research (NIPR).

Station	Country	Geographic (deg)		Geomagnetic (deg)		MLT
		Latitude	Longitude	Latitude	Longitude	
INTERMAGNET https://www.intermagnet.org/data-donnee/download-eng.php						
Uppsala UPS	Sweden	59.90N	17.35E	58.5N	106.35E	UT+1.75
Memambetsu MMB	Japan	43.91N	144.19E	35.72N	147.77W	UT+9.4
Hermanus HER	South Africa	34.42S	19.23E	33.95S	83.87 E	UT+0.82
Learmonth LRM	Australia	22.22S	114.10E	32.51S	186.35E	UT+7.69
World Data Centre for Geomagnetism, Mumbai (http://wdciig.res.in/WebUI/Home.aspx)						
Alibag ABG	India	18.64N	72.87E	10.76N	146.90E	UT+5.01
Tirunelveli TIR	India	8.70N	77.80E	0.52N	150.83E	UT+5.30
NIPR http://polaris.nipr.ac.jp/~uap-mon/uapm/uapm_new_top.html						
Tjornes TJO	Iceland	66.20N	17.12W	66.53N	72.30E	UT-0.28
Syowa SYO	Antarctica	69.00S	39.58E	70.46S	86.10E	UT-0.33

magnetosphere (Tanaka, 2007; Ebihara et al., 2014; Tanaka et al., 2020). The physical basis for the instantaneous propagation of the electric potential and currents in the potential solver is provided by the TM_0/TEM waveguide/transmission line mode.

OBSERVATION FACILITIES

Magnetometer Networks

The SC was recorded at middle latitudes in the northern hemisphere; Uppsala (UPS, 58.50°N geomagnetic latitude (GML)) in the morning (8.4 MLT) and Memambetsu (MMB, 35.72°N GML) in the afternoon (16.3 MLT). In the southern hemisphere, the SC was recorded at Hermanus (HER, 33.95°S GML) in the morning (7.5 MLT) and Learmonth (LRM, 32.51°S GML) in the afternoon (14.3 MLT). We used low latitude and equatorial stations; Alibag (ABG, 10.76°N GML) and Tirunelveli (TIR, 0.52°N GML) at noon (12 MLT) to confirm the Pedersen–Cowling current circuit. We also used the conjugate stations at auroral latitudes in the northern and southern hemispheres; Tjornes (TJO, 66.53°N GML) and Syowa (SYO, 70.46°S GML), to detect ionospheric currents near the FACs in the morning (6.5 MLT). The magnetometer data were sampled every 1 s at TJO, SYO, MMB, HER, and LRM, and 10 s at UPS. The magnetometer stations are listed in **Table 1**.

HF Doppler Sounder Networks

The HF Doppler sounders were operated at Kasperk, Czechia (48.67°N GML), and Iitate, Sugadaira, Fujisawa, in Japan (27–29.5°N GML), as listed in **Table 2**, to detect the vertical motion of the ionosphere due to the electric fields of SC in the morning (0730 MLT) and afternoon (1530 MLT), respectively. The HF Doppler sounder system is composed of the transmitter (Tx) and receiver (Rx) separated at distances listed in **Table 2**. The HF Doppler sounder system in Czechia is composed of three transmitters (Tx1, Tx2, and Tx3) with a frequency of 4.65 MHz and one receiver (Rx) at distances 118–171 km, as shown in **Table 2**, where the elevation angle is for reflection height of 300 km. Details of the system and the

principle of Doppler sounding are described by Chum et al. (2010). The HF Doppler sounder system in Japan is composed of Tx in Tokyo with frequencies of 5.006 and 8.006 MHz and several receivers deployed from the northernmost part (Hokkaido) to the southernmost part (Okinawa) of Japan. Details of the system in Japan are described by Nakata et al. (2021). The receiver sites and frequency used in the present analyses are listed in **Table 2**. The data are sampled every 6 s in Czechia and 10 s in Japan. The time resolutions of the HF Doppler data are high enough to detect the PI and MI electric fields (Kikuchi et al., 2016; Kikuchi et al., 2021).

GEOMAGNETIC SUDDEN COMMENCEMENT AT MIDDLE LATITUDES IN THE NORTHERN AND SOUTHERN HEMISPHERES

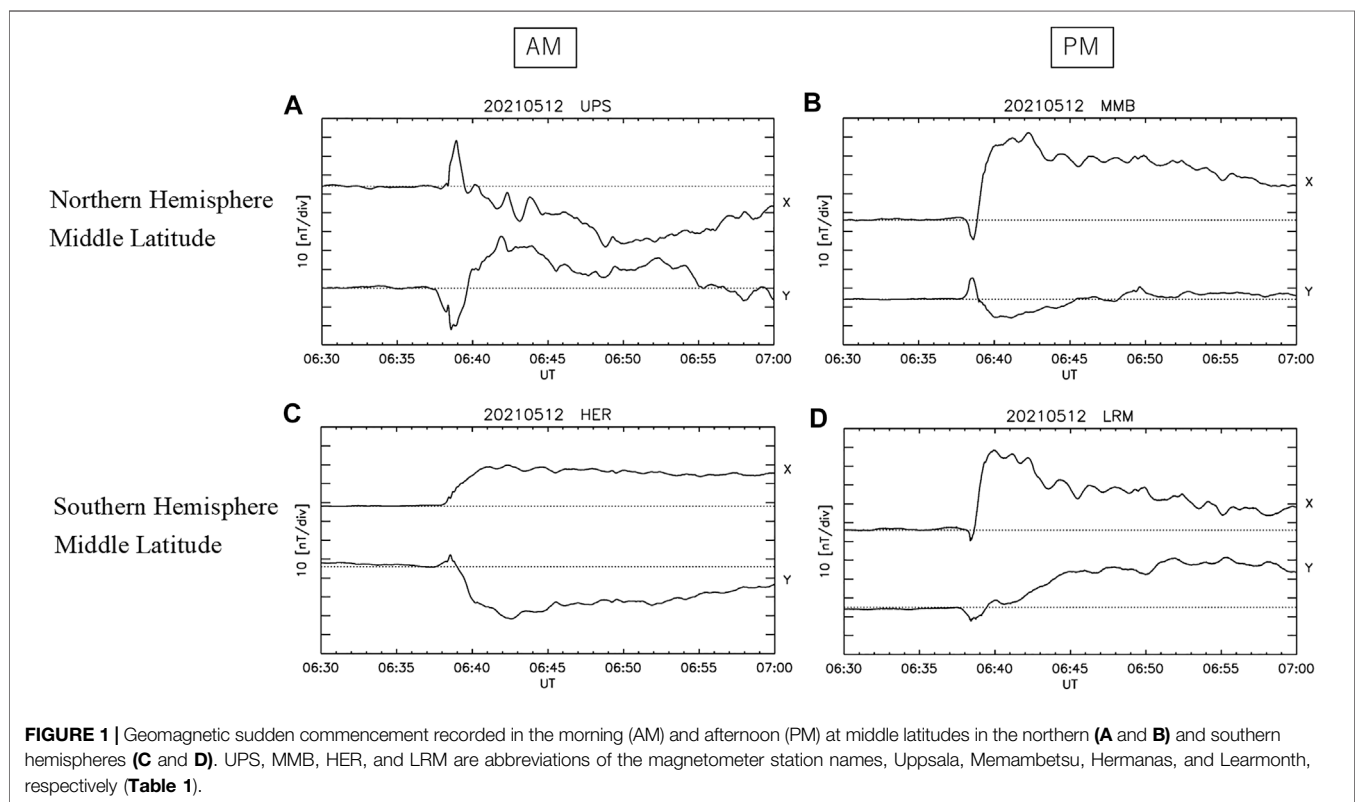
Figures 1A and B show SC_x (+ -) and SC_y (- +) at UPS in the morning (**Figure 1A**) and SC_x (- +) and SC_y (+ -) at MMB in the afternoon (**Figure 1B**), showing morning/afternoon asymmetry both in SC_x and SC_y in the northern hemisphere. SC_x agrees with Araki (1994)'s model composed of the PI_x and MI_x superimposed on the step-like DL. The morning/afternoon asymmetry in PI_x agrees with the two-cell Hall current vortices with counter-clockwise and clockwise directions in the morning and afternoon, respectively (see the schematic current circuit in **Figure 6**). The morning/afternoon asymmetry in PI_y agrees with the northward and southward Pedersen currents in the morning and afternoon, respectively. The morning/afternoon asymmetry in MI_x is explained by similar current circuits with reverse direction.

Figures 1C and D show SC_x (+ +) and SC_y (+ -) at HER in the morning (**Figure 1C**) and SC_x (- +) and SC_y (- +) at LRM in the afternoon (**Figure 1D**), showing the morning/afternoon asymmetry both in SC_x and SC_y in the southern hemisphere, although B_x at HER is not sensitive to the PI/MI currents. The SC_x at HER is almost DL, but SC_y is clearly identified as SC_y (+ -).

It is observed that the SC_x at LRM is in the same polarity as SC_x at MMB, while SC_y in the southern hemisphere is in opposite

TABLE 2 | List of HF Doppler sounders in Japan [HF Doppler Sounding Experiment in Japan (uec.ac.jp)] and Czechia [Doppler sounding of the Ionosphere (cas.cz)].

Station name	Country	Frequency (MHz)	Geographic coordinate (deg)		Geomagnetic coordinate (deg)		Tx-Rx distance (km)	Elevation angle (deg)
			Latitude	Longitude	Latitude	Longitude		
litate IIT	Japan	8.006	37.69	140.67	29.53	-149.92	248	67.5
Sugadaira SGD	Japan	8.006	36.52	138.32	27.89	-152.06	147	76.2
Fujisawa FJS	Japan	8.006	35.32	139.46	27.08	-150.76	37.6	86.4
Kasperk	Czechia	4.65	49.13	13.58	48.67	96.98	171 (Tx1) 118 (Tx2) 169 (Tx3)	74.1 78.9 74.3

**FIGURE 1** | Geomagnetic sudden commencement recorded in the morning (AM) and afternoon (PM) at middle latitudes in the northern (A and B) and southern hemispheres (C and D). UPS, MMB, HER, and LRM are abbreviations of the magnetometer station names, Uppsala, Memambetsu, Hermanas, and Learmonth, respectively (Table 1).

polarity to SC_y in the northern hemisphere in both the morning and afternoon. The SC_x in the southern hemisphere except for SC_x (+ +) at HER matches the two-cell Hall current vortices that are mirror images of the Hall current vortices in the northern hemisphere. The SC_y in the southern hemisphere matches the Pedersen currents that are mirror images of those in the northern hemisphere (Figure 6).

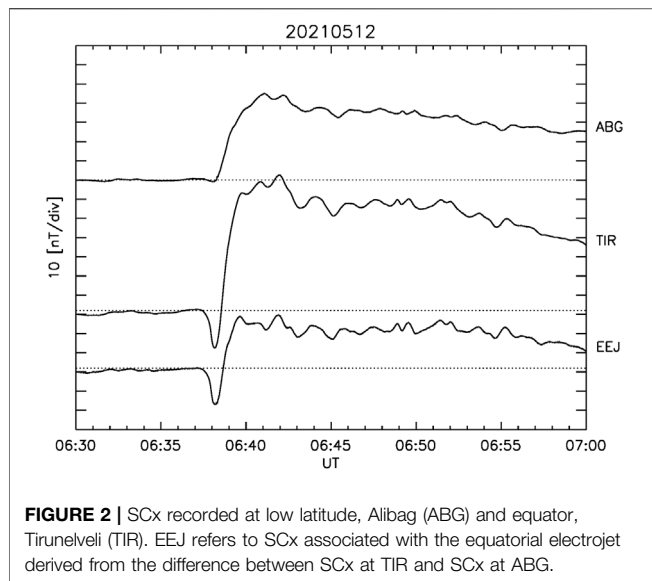
SC AT LOW LATITUDE AND THE EQUATOR

Figure 2 shows SC_x at low latitude, Alibag (ABG, 10.76° GML) and the equator, Tirunelveli (TIR, 0.52° GML), located at noon (11.9 MLT) together with the EEJ defined as the difference in B_x between TIR and ABG. The SC_x at ABG is a step-like increase, which is a typical DL caused by the magnetopause current. The SC_x at TIR is

SC_x (- +), which is typical at the equator on the dayside (Araki, 1994). The Pedersen currents responsible for the midlatitude PI_y connect to the Cowling currents responsible for the PI_x at TIR, completing a Pedersen–Cowling current circuit between high latitude and equator (Figure 6). Likewise, midlatitude MI_y is caused by the Pedersen current circuit between the MI FACs and the Cowling currents with opposite directions to those of PI.

SIMULTANEOUS ONSET OF PI IN THE NORTHERN AND SOUTHERN HEMISPHERES

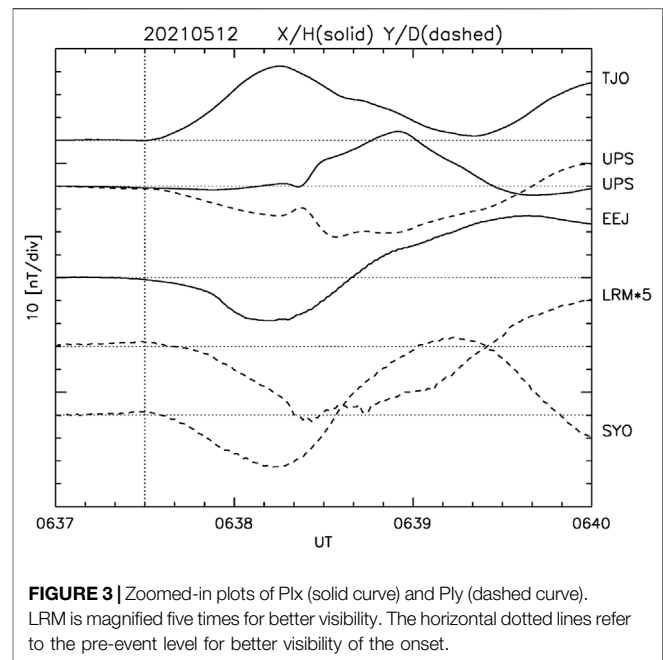
Figure 3 shows zoomed-in plots of the PI at high latitude–equatorial stations in a 3-min time frame where one increment is 10 s. To show



the clear onset of the PI, we plotted B_x at TJO and EEJ with solid curves and B_y at UPS, LRM, and SYO with dashed curves, where LRM is magnified five times for better visibility. We also plotted B_x at UPS to show that the onset of PI_x can be delayed, as will be discussed later. The PI_x/PI_y starts at 0637:30 s UT (vertical dotted line) at all the stations within the resolution of a few seconds. It is remarkable that the onset of the PI is simultaneous at the conjugate auroral stations (TJO, SYO) and at the midlatitude and equatorial stations. The observations meet the instantaneous development of ionospheric Hall and Pedersen–Cowling currents from high latitude to the equator, which is achieved by the TM_0/TEM mode waves propagating at the speed of light in the Earth-ionosphere waveguide/transmission line (Kikuchi et al., 1978; Kikuchi and Araki, 1979; Kikuchi, 2014).

HF DOPPLER OBSERVATIONS OF THE SC ELECTRIC FIELDS

Figure 4 shows the SC-associated HF Doppler frequencies (SCF) observed at Kasperk, Czechia, in the morning and at Iitate, Sugadaira, Fujisawa, Japan, in the afternoon. Three SCFs at Kasperk were obtained from HF radio signals transmitted by three transmitters, Tx1, Tx2, and Tx3, as received at one receiver (**Table 2**). The SCF is SCF (+ -) in both the morning and afternoon, composed of the positive PFD with a duration of 1 min and negative MFD with a duration of 4 min. The PFD and MFD are caused by the westward and eastward electric fields, that is, the dayside part of the dusk-to-dawn and dawn-to-dusk electric fields of the PI and MI, respectively. These electric fields drive the Hall current vortices responsible for the PI_x and MI_x at UPS and MMB. It should be stressed that the PFD is caused by the potential electric field transmitted with the Pedersen currents responsible for the equatorial PI (Kikuchi et al., 2016). The onset of the PFD at Kasperk is 0637:30UT, the same as the PI of global currents (**Figure 3**). The onset of the PFD cannot be identified very

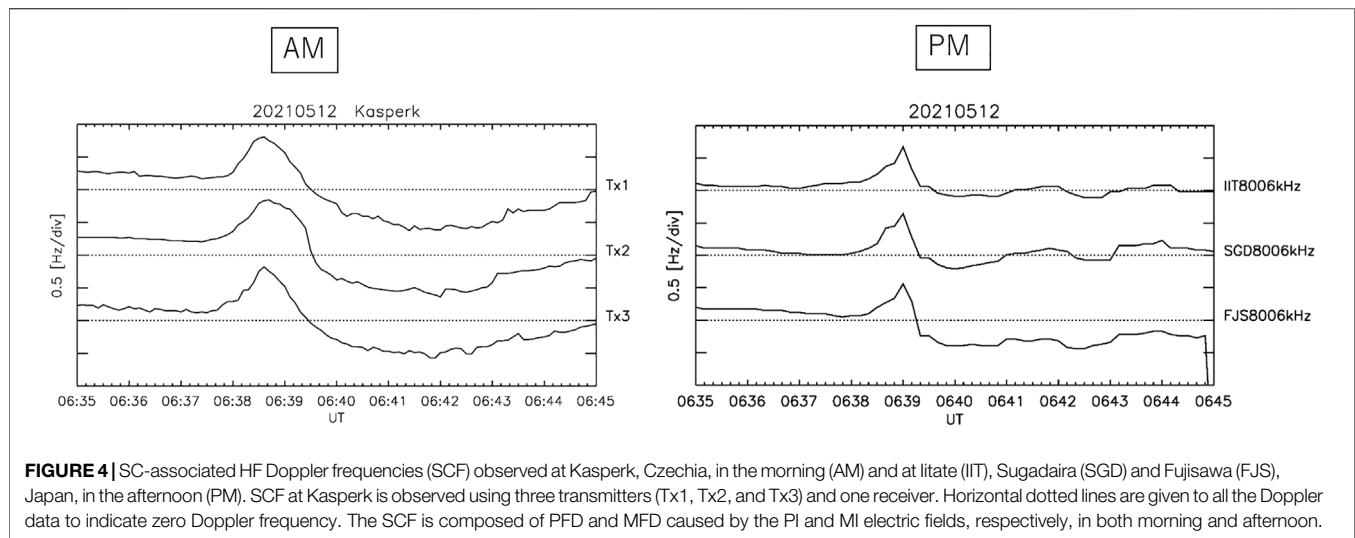


clearly at stations in the afternoon, which may be due to ionospheric conditions over Japan.

REPRODUCTION OF SC BY GLOBAL SIMULATION

We reproduced SC electric fields at the middle latitude and magnetic field due to the Cowling currents using the REPPU (REProduce Plasma Universe) global simulation model, where the current continuity equation is solved in the anisotropic and inhomogeneous conducting ionosphere at the inner boundary (2.6 Re) of the magnetosphere (Tanaka et al., 2020). At the simulation boundary upstream in the solar wind, the IMF B_z changes from +3 nT to -5 nT and solar wind speed from 300 to 500 km/s in the form of a step function. The solar wind density and IMF B_y are constant at 5/cc and 2.5 nT, respectively (Ebihara et al., 2014). **Figures 5A and B** show the electric fields for Kasperk (**Figure 5A**) and Japanese stations (**Figure 5B**). The reproduced electric fields in the morning and afternoon are in good agreement with the observed SCF (**Figure 4**) in terms of time scale and polarity (note that Doppler frequency is positive for westward electric field). The good agreement between the simulation and observations suggests that the PI and MI electric fields are potential fields associated with ionospheric currents.

Figure 5C shows the reproduced equatorial SCx (- +) caused by the Cowling currents at 12 MLT, which is consistent with the SCx (- +) observed at TIR (**Figure 2**). In the model calculation where the current continuity equation is employed, instantaneous propagation of the electric field and currents is a priori assumed. The speed of light propagation of the TM_0/TEM mode waves provides a physical basis for the instantaneous propagation in the model ionosphere.



SUMMARY AND DISCUSSION

Hall and Pedersen Current Circuits

Figure 6 shows a schematic diagram of the ionospheric current circuits that explain the global characteristics of the observed PI in the northern and southern hemispheres and at the equator on the dayside. The ionospheric current circuits are composed of two-cell Hall current vortices at high and middle latitudes (orange circles) and the Pedersen currents (blue semicircles) extending from the foot of FACs (thick blue arrows) to the equatorial Cowling currents (black arrow). The two-cell current vortices of the PI were described as the equivalent currents estimated from ground magnetic variations (Nagata and Abe, 1955). The ionospheric current pattern is supposed to be affected by the ionospheric conductivities, particularly at auroral latitudes, where the foot of FACs is located and ionospheric conductivities are enhanced by precipitating auroral particles. However, the SC most often occurs during quiet periods prior to stormtime disturbances, as is the case on 12 May 2021, which would allow us to use the simplified two-cell Hall current vortices as shown in **Figure 6**. The current circuits in the northern and southern hemispheres are mirror images of each other, so the following discussion applies to the northern hemisphere.

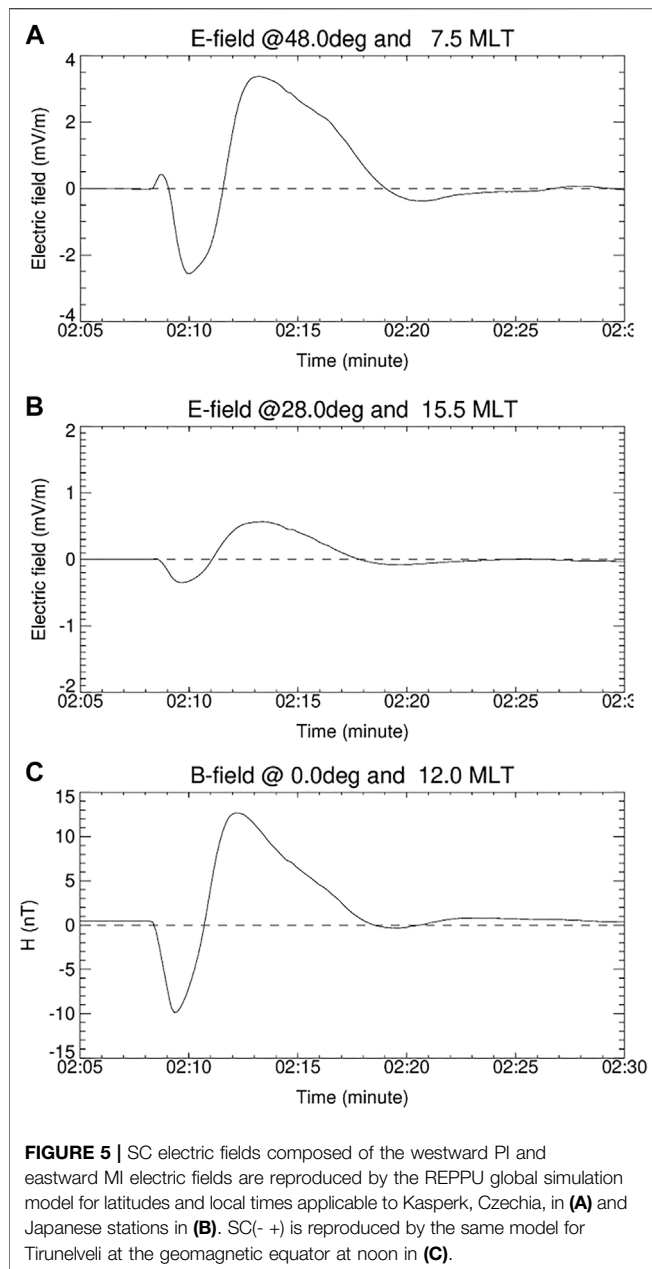
The pair of FACs of the PI provides electric potentials to the polar ionosphere from the dynamo created by the compression of the magnetosphere (Tamao, 1964a; Tamao, 1964b; Slinker et al., 1999; Fujita et al., 2003a). The electric potentials are then transmitted with the Pedersen currents to the global ionosphere by the TM_0/TEM mode wave in the Earth-ionosphere waveguide/transmission line (Kikuchi, 2014). The magnetic field of the TM_0 mode propagating equatorward is negative/positive B_y , and the Pedersen currents are northward/southward in the morning/afternoon. The disseminated potential electric fields drive counterclockwise/clockwise Hall current vortices closing around the upward/downward FACs in the morning/afternoon, as shown in **Figure 6**. The Hall current vortices

cause positive/negative PI_x as observed at middle latitudes in the morning/afternoon (**Figure 1**). The upward/downward FACs are connected to the equatorial ionosphere in the morning/afternoon *via* the northward/southward Pedersen currents, which cause the negative/positive PI_y as observed at middle latitudes (**Figure 1**). The Pedersen–Cowling current circuit is achieved near-instantaneously, causing the negative PI_x at the dayside equator (**Figure 2**).

Simultaneous Onset of PI

We found that the onset of PI_y is simultaneous with the temporal resolution of a few seconds in both the northern and southern hemispheres, even when PI_x is delayed by tens of seconds, as seen in PI_x at UPS in **Figure 3**. The delay could be due to the fact that the Pedersen current had a westward component and canceled the Hall current effect. The instantaneous transmission of the electric potentials is achieved by the TM_0/TEM mode waves in the Earth-ionosphere waveguide/transmission line, which carries the Pedersen currents together with ground surface currents connected by the wave front currents (Kikuchi, 2014). We stress that the B_y component is associated with the TM_0/TEM mode propagating southward, which helps confirm the simultaneous onset of the global PI_y .

Concerning the instantaneous propagation from high latitude to low latitude of the electric field/magnetic field, lots of studies have used the fast (compressional) mode waves propagating at the Alfvén speed perpendicular to the ambient magnetic field in the upper ionosphere (Tu and Song, 2019) or the Alfvén waves converted from the compressional mode (Tamao, 1964a; Tamao, 1964b; Chi et al., 2006). However, no theory/model based on the fast mode waves has succeeded to explain the Hall and Pedersen–Cowling current circuits responsible for the PI and MI on the ground. Tamao (1964b) attempted to explain the Hall current vortices by means of the converted transverse mode (CT mode) converted from the compressional mode at its wave front. It should be recalled that the Hall current is a result of ion-neutral collisions in the ionospheric E-layer, which decouple the ion



motion from that of the collision-free electrons and create the Pedersen currents as well. Therefore, a theory/model that aims for explaining the Hall current circuits should also explain the Pedersen current circuits. The CT mode never carries FACs, since the electric field of the CT mode is solenoidal (rotational) (Tamao, 1964b), so the Pedersen currents are not supplied by the CT mode or by the compressional mode. Kikuchi (2014) showed that the TM_0/TEM mode transports electric potentials and the Pedersen currents from the foot of the FACs to the Cowling currents *via* the midlatitude. The TM_0/TEM mode does not have the cutoff frequency of the waveguide, which allows any period of disturbances such as the SC, DP2 and so on. It should be noted that the Schumann resonance frequency at about 8 Hz is misunderstood as the lower cutoff frequency of the Earth-

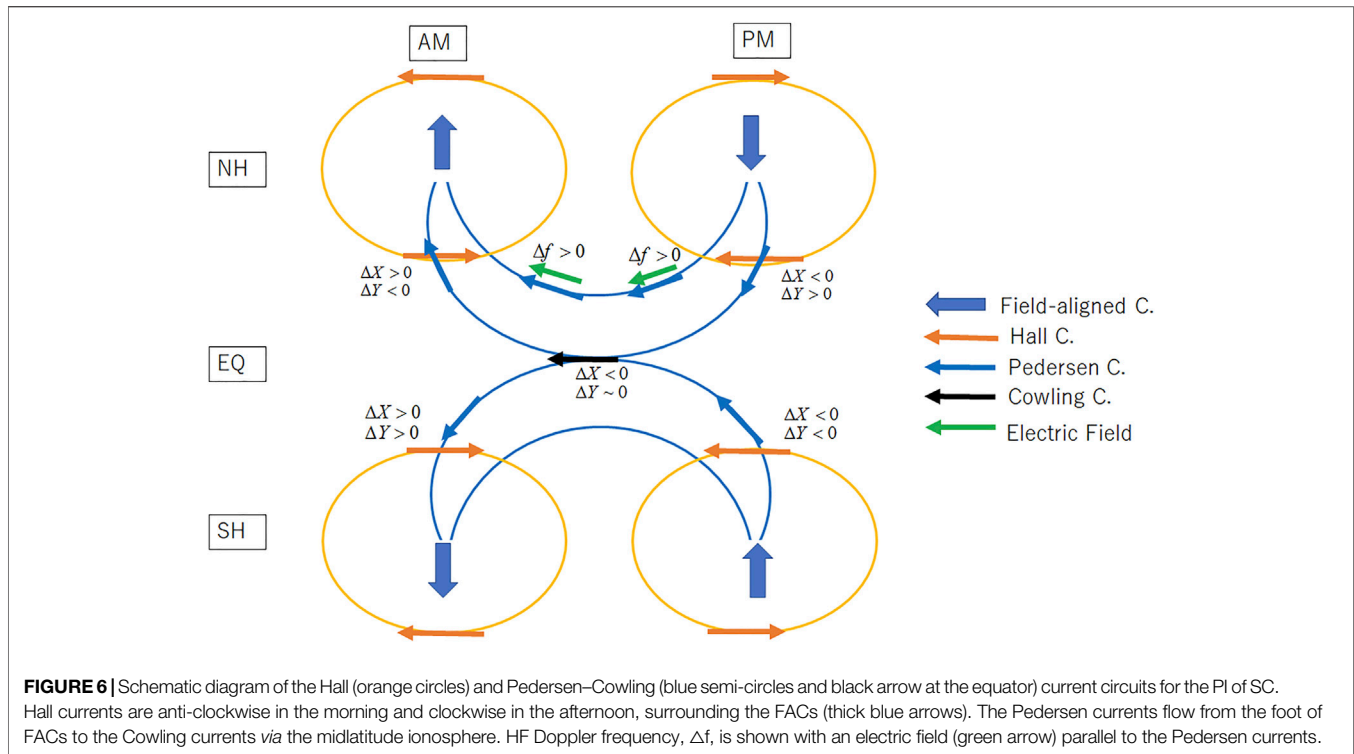
ionosphere waveguide (Lysak et al., 2015). The Schumann resonance is a global cavity resonance created by the propagating TM_0 mode waves in the Earth-ionosphere waveguide (Wait, 1960). Wait (1960) describes that “Schumann [1956] has carried out an extensive set of calculations of waveforms for the zero mode in the idealized Earth-ionosphere waveguide”. The TM_0 waveguide mode is the TEM transmission line mode that is unattenuated at all frequencies (Budden, 1961, p33). It should also be noted that the plasma motion observed by HF Doppler sounders is upward on the dayside during the MI phase of an SC event which is well correlated with the eastward Cowling currents (Kikuchi et al., 2016). This fact indicates that the ionospheric plasma is never compressed by the compressional mode wave but is moved by the electric field transmitted with the Pedersen currents. It should be stressed that the theory/model designed to explain the fast propagation of electric and magnetic fields to low latitude should also explain the energy supply to the Pedersen and Cowling currents.

HF Doppler Observation of SC Electric Fields

The HF Doppler sounders detected downward motion of the ionospheric plasma for the first 1 min, followed by the upward motion for 4 min in both the morning and afternoon (Figure 4). The initial downward motion was interpreted as caused by the compressional wave (Huang, 1976; Pilipenko et al., 2010). The magnetospheric plasma is compressed earthward during the SC, as observed by the Akebono satellite (Shinbori et al., 2004). However, Kikuchi et al. (2016) showed that the dayside ionosphere never moves earthward (downward) but moves upward as the eastward Cowling current grows during the MI phase when the magnetosphere continues to be compressed. The electric field responsible for the upward motion is not the electric field of the compressional wave but is the potential field associated with the ionospheric Pedersen/Cowling current. The initial downward motion in Figure 4 occurred during the period of the equatorial PI caused by the westward Cowling current (Figure 2), which indicates that the PI electric field at middle latitude is transmitted by the TM_0/TEM mode in the Earth-ionosphere waveguide/transmission line.

Application to Pi2 Pulsation

Tsunomura (1998) showed that the midlatitude MIy is positive in the morning and negative in the afternoon, and its amplitude is larger at higher latitudes. These observations meet the Pedersen current circuit, as shown in Figure 6. The latitudinal variation of MIx, on the other hand, is not so significant, implying that MIx is superimposed by DL. A similar difference in the latitudinal profiles between B_x and B_y was found for Pi2 magnetic pulsation, of which period (1 min) is the same as the time scale of PI (Yumoto et al., 1994). Yumoto et al. (1994) showed that Pi2 in the B_y component is in an anti-phase relationship in the northern and southern hemispheres, and the amplitude increases exponentially at higher latitudes. Imajo et al. (2015), Imajo et al. (2017) made detailed analyses of Pi2 in B_y and



suggested that the anti-phase relationship is caused by ionospheric currents that are symmetric with respect to the equator. The latitudinal and hemispheric characteristics of PI_2 are similar to those of PI_y and MI_y reported in the present article, consistent with the Pedersen–Cowling current circuit as depicted in **Figure 6**.

CONCLUSION

We analyzed the geomagnetic sudden commencement (SC) on 12 May 2021 with magnetometer data recorded in the morning and afternoon at high and middle latitudes in the northern and southern hemispheres and at the noontime equator. The electric field of the SC was observed by the HF Doppler sounders at middle latitudes in the morning and afternoon in the northern hemisphere. Local time, latitude, and hemispheric characteristics are obtained as follows.

- 1) SC in B_x - and B_y -components are SC_x (+ -) and SC_y (- +) in the morning and SC_x (- +) and SC_y (+ -) in the afternoon at middle latitudes in the northern hemisphere. SC_x in the southern hemisphere has the same polarity as those in the northern hemisphere except for SC_x (+ +) in the morning, while SC_y in the southern hemisphere has reverse polarity to those in the northern hemisphere.
- 2) Preliminary impulse in B_x (PI_x) in the northern hemisphere matches the conventional two-cell Hall current vortices with anti-clockwise and clockwise directions in the morning and afternoon, respectively, and the MI_x matches reverse Hall current vortices. PI_x and MI_x in the southern hemisphere meet the Hall current vortices that are mirror images of those in the northern hemisphere with respect to the equator.
- 3) PI_y in the northern hemisphere is found to meet the northward and southward Pedersen currents in the morning and afternoon, respectively, and the MI_y meets reverse Pedersen currents. The PI_y and MI_y in the southern hemisphere are found to meet the Pedersen currents that are mirror images of those in the northern hemisphere.
- 4) At the equator, typical SC_x (- +) is observed, meeting the Cowling currents supplied by the Pedersen currents from the northern and southern hemispheres.
- 5) The electric fields of the PI and MI observed by the HF Doppler sounders at the middle latitudes in the northern hemisphere are westward and eastward, respectively, in both the morning and afternoon, meeting the conventional model composed of dusk-to-dawn PI and dawn-to-dusk MI potential electric fields.
- 6) The onset of the PI_x/PI_y is found to be simultaneous with the resolution of a few seconds in both the northern and southern hemispheres, indicating instantaneous achievement of the Hall and Pedersen–Cowling current circuits by the TM_0/TEM mode wave propagating at the speed of light in the Earth-ionosphere waveguide/transmission line.
- 7) REPPU global simulation model reproduces the PI and MI electric fields at middle latitudes and SC_x (- +) at the dayside equator. The simulation results are found to be consistent with most features of observations, such as the time scale of PI and MI, direction of the midlatitude electric field, and generation of equatorial Cowling currents. The simulation proves that the

ionospheric electric fields are potential fields transmitted in the Pedersen–Cowling current circuit.

DATA AVAILABILITY STATEMENT

Publicly available datasets were analyzed in this study. This data can be found at 1. HF Doppler: HF Doppler Sounding Experiment in Japan-HFDOPE, The University of Electro-Communications (<http://gwave.cei.uec.ac.jp/~hfd/>) 2. HF Doppler. The Institute of Atmospheric Physics of the Czech Academy of Science, (<http://datacenter.ufa.cas.cz/>) 3. Magnetometer data: World Data Center for Geomagnetism, Kyoto (<http://wdc.kugi.kyoto-u.ac.jp/wdc/Sec3.html>) 4. Magnetometer data: Kakioka Magnetic Observatory (<http://www.kakioka-jma.go.jp/obsdata/metadata/en>) 5. Magnetometer data: World Data Centre for Geomagnetism, Mumbai (<http://wdciig.res.in/WebUI/Home.aspx>) Us | Indian Institute of Geomagnetism (IIG) (iigm.res.in) 6. Magnetometer data: Data Center for Aurora, National Institute of Polar Research polaris.nipr.ac.jp/~uap-mon/uapm/uapm_new_top.html 7. Magnetometer data: INTERMAGNET website (<http://www.intermagnet.org>).

AUTHOR CONTRIBUTIONS

TK and KKH analyzed the magnetometer and HF Doppler data for the SC event. TA and YN provided ideas about the global current circuits. YE and TT performed global simulations of SC electric field and currents. GV and AS performed magnetometer observations in India and provided suggestions on the onset of PI at the equator. JC performed HF Doppler observations in Czechia. KH and IT performed HF Doppler observations in Japan. YT and AK performed magnetometer observations at TJO and SYO.

REFERENCES

- Araki, T., Allen, J. H., and Araki, Y. (1985). Extension of a Polar Ionospheric Current to the Nightside Equator. *Planet. Space Sci.* 33, 11–16. doi:10.1016/0032-0633(85)90137-0
- Araki, T., Keika, K., Kamei, T., Yang, H., and Alex, S. (2006). Nighttime Enhancement of the Amplitude of Geomagnetic Sudden Commencements and its Dependence on IMF-Bz. *Earth Planet Sp.* 58, 45–50. doi:10.1186/bf03351912
- Araki, T. (1977). Global Structure of Geomagnetic Sudden Commencements. *Planet. Space Sci.* 25, 373–384. doi:10.1016/0032-0633(77)90053-8
- Araki, T. (1994). A Physical Model of the Geomagnetic Sudden Commencement, Solar Wind Sources of Magnetospheric Ultra-low-frequency Waves. *Geophys. Monogr.* 81, 183–200.
- Baker, W. G., and Martyn, D. F. (1953). Electric Currents in the Ionosphere I. The Conductivity. *Phil. Trans. R. Soc. Lond. Ser. A* 246, 281–294.
- Budden, K. G. (1961). *The Wave-Guide Mode Theory of Wave Propagation*. Academic Press Inc. London, 33–34.
- Chi, P. J., Lee, D.-H., and Russell, C. T. (2006). Tamao Travel Time of Sudden Impulses and its Relationship to Ionospheric Convection Vortices. *J. Geophys. Res.* 111, A08205. doi:10.1029/2005JA011578
- Chum, J., Šindelářová, T., Laštovička, J., Hruška, F., Burešová, D., and Baše, J. (2010). Horizontal Velocities and Propagation Directions of Gravity Waves in the Ionosphere over the Czech Republic. *J. Geophys. Res.* 115. doi:10.1029/2010JA015821

FUNDING

This study is supported by the grants-in-aid for Scientific Research (15H05815, 20H01960) of Japan Society for the Promotion of Science (JSPS) and by JSPS KAKENHI Grant Number JP22540461 and JP26400481. The works of TK are supported by the joint research program of the Institute for Space-Earth Environmental Research, Nagoya University, the KDK of the Research Institute for Sustainable Humanosphere, Kyoto University, and National Institute of Polar Research, Tokyo. The work of JC was supported under the grant 18-01969S by the Czech Science Foundation. The works of IT, KKH, KH, and TK are supported by Hosono Bunka Foundation, the Takahashi Industrial and Economic Research Foundation and the Murata Science Foundation. The works of YN is supported by NASA Grant 80NSSC18K0657, 80NSSC20K0604, 80NSSC20K0725, 80NSSC21K1321, and 80NSSC20K1788, NSF Grant AGS-1907698 and AGS-2100975, and AFOSR Grant FA9559-16-1-0364.

ACKNOWLEDGMENTS

The results presented in this article rely on the data collected at Hermanus, Uppsala, Learmonth and Memambetsu. The authors thank the South African National Space Agency (SANSA) for data from Hermanus, Uppsala Geological Survey of Sweden (SGU) for Uppsala, Geoscience Australia (GA) for Learmonth and Kakioka Magnetic Observatory, and Japan Meteorological Agency (JMA) for Memambetsu. The authors thank INTERMAGNET for promoting high standards of magnetic observatory practice (www.intermagnet.org). The authors also thank the National Institute of Polar Research for data from Tjornes and Syowa and the Indian Institute of Geomagnetism for Alibag and Tirunelveli.

- Ebihara, Y., Tanaka, T., and Kikuchi, T. (2014). Counter Equatorial Electrojet and Overshielding after Substorm Onset: Global MHD Simulation Study. *J. Geophys. Res. Space Phys.* 119, 7281–7296. doi:10.1002/2014JA020065
- Fujita, S., Tanaka, T., Kikuchi, T., Fujimoto, K., Hosokawa, K., and Itonaga, M. (2003a). A Numerical Simulation of the Geomagnetic Sudden Commencement: 1. Generation of the Field-Aligned Current Associated with the Preliminary Impulse. *J. Geophys. Res.* 108 (A12), 1416. doi:10.1029/2002JA009407
- Fujita, S., Tanaka, T., Kikuchi, T., Fujimoto, K., and Itonaga, M. (2003b). A Numerical Simulation of the Geomagnetic Sudden Commencement: 2. Plasma Processes in the Main Impulse. *J. Geophys. Res.* 108 (A12), 1417. doi:10.1029/2002JA009763
- Hirono, M. (1952). A Theory of Diurnal Magnetic Variations in Equatorial Regions and Conductivity of the Ionosphere E Region. *J. Geomagn. Geoelec.* 4, 7–21. doi:10.5636/jgg.4.7
- Huang, Y.-N., Najita, K., and Yuen, P. (1973). The Ionospheric Effects of Geomagnetic Sudden Commencements as Measured with an HF Doppler Sounder at Hawaii. *J. Atmos. Terr. Phys.* 35, 173–181. doi:10.1016/0021-9169(73)90225-0
- Huang, Y.-N. (1976). Modeling HF Doppler Effects of Geomagnetic Sudden Commencements. *J. Geophys. Res.* 81, 175–182. doi:10.1029/ja081i001p00175
- Imajo, S., Yoshikawa, A., Uozumi, T., Ohtani, S., Nakamizo, A., Marshall, R., et al. (2015). Pi2 Pulsations Observed Around the Dawn Terminator. *J. Geophys. Res. Space Phys.* 120, 2088–2098. doi:10.1002/2013JA019691
- Imajo, S., Yoshikawa, A., Uozumi, T., Ohtani, S., Nakamizo, A., and Chi, P. J. (2017). Application of a Global Magnetospheric-ionospheric Current Model for

- Dayside and Terminator Pi2 Pulsations. *J. Geophys. Res. Space Phys.* 122, 8589–8603. doi:10.1002/2017JA024246
- Kikuchi, T., and Araki, T. (1979). Horizontal Transmission of the Polar Electric Field to the Equator. *J. Atmos. Terr. Phys.* 41, 927–936. doi:10.1016/0021-9169(79)90094-1
- Kikuchi, T., Araki, T., Maeda, H., and Maekawa, K. (1978). Transmission of Polar Electric Fields to the Equator. *Nature* 273, 650–651. doi:10.1038/273650a0
- Kikuchi, T., Ishimine, T., and Sugiuchi, H. (1985). Local Time Distribution of HF Doppler Frequency Deviations Associated with Storm Sudden Commencements. *J. Geophys. Res.* 90, 4389–4393. doi:10.1029/ja090ia05p04389
- Kikuchi, T., Hashimoto, K. K., Tomizawa, I., Ebihara, Y., Nishimura, Y., Araki, T., et al. (2016). Response of the Incompressible Ionosphere to the Compression of the Magnetosphere during the Geomagnetic Sudden Commencements. *J. Geophys. Res. Space Phys.* 121, 1536–1556. doi:10.1002/2015ja022166
- Kikuchi, T., Chum, J., Tomizawa, I., Hashimoto, K. K., Hosokawa, K., Ebihara, Y., et al. (2021). Penetration of the Electric Fields of the Geomagnetic Sudden Commencement over the Globe as Observed with the HF Doppler Sounders and Magnetometers. *Earth Planets Space* 73. doi:10.1186/s40623-020-01350-8
- Kikuchi, T. (1986). Evidence of Transmission of Polar Electric Fields to the Low Latitude at Times of Geomagnetic Sudden Commencements. *J. Geophys. Res.* 91, 3101–3105. doi:10.1029/ja091ia03p03101
- Kikuchi, T. (2014). Transmission Line Model for the Near-Instantaneous Transmission of the Ionospheric Electric Field and Currents to the Equator. *J. Geophys. Res. Space Phys.* 119, 1131–1156. doi:10.1002/2013JA019515
- Lysak, R. L., Song, Y., Sciffer, M. D., and Waters, C. L. (2015). Propagation of Pi2 Pulsations in a Dipole Model of the Magnetosphere. *J. Geophys. Res. Space Phys.* 120, 355–367. doi:10.1002/2014JA020625
- Nagata, T., and Abe, S. (1955). Notes on the Distribution of SC* in High Latitudes. *Rept. Ionos. Res. Jpn.* 9, 39–44.
- Nakata, H., Nozaki, K., Oki, Y., Hosokawa, K., Hashimoto, K. K., Kikuchi, T., et al. (2021). Software-defined Radio-Based HF Doppler Receiving System. *Earth Planets Space* 73. doi:10.1186/s40623-021-01547-5
- Nilam, B., Ram, S. T., Shiokawa, K., Balan, N., and Zhang, Q. (2020). The Solar Wind Density Control on the Prompt Penetration Electric Field and Equatorial Electrojet. *J. Geophys. Res. Space Phys.* 125, e2020JA027869. doi:10.1029/2020JA027869
- Pilipenko, V., Fedorov, E., Yumoto, K., Ikeda, A., and Sun, T. R. (2010). An Analytical Model for Doppler Frequency Variations of Ionospheric HF Sounding Caused by SSC. *J. Geophys. Res.* 115. doi:10.1029/2010JA015403
- Rastogi, R. G., Pathan, B. M., Rao, D. R. K., Sastry, T. S., and Sastri, J. H. (2001). On Latitudinal Profile of Storm Sudden Commencement in H, Y and Z at Indian Geomagnetic Observatory Chain. *Earth Planet Sp.* 53, 121–127. doi:10.1186/BF03352369
- Rastogi, R. G. (1993). Longitudinal Variation of Sudden Commencement of Geomagnetic Storm at Equatorial Stations. *J. Geophys. Res.* 98, 15,411–15,416. doi:10.1029/92ja02971
- Sastri, J. H. (2002). Penetration Electric Fields at the Nightside Dip Equator Associated with the Main Impulse of the Storm Sudden Commencement of 8 July 1991. *J. Geophys. Res.* 107 (A12), 9–1. doi:10.1029/2002JA009453
- Shinbori, A., Ono, T., Iizima, M., and Kumamoto, A. (2004). SC Related Electric and Magnetic Field Phenomena Observed by the Akebono Satellite inside the Plasmasphere. *Earth Planet Sp.* 56, 269–282. doi:10.1186/bf03353409
- Shinbori, A., Tsuji, Y., Kikuchi, T., Araki, T., and Watari, S. (2009). Magnetic Latitude and Local Time Dependence of the Amplitude of Geomagnetic Sudden Commencements. *J. Geophys. Res.* 114. doi:10.1029/2008JA013871
- Slinker, S. P., Fedder, J. A., Hughes, W. J., and Lyon, J. G. (1999). Response of the Ionosphere to a Density Pulse in the Solar Wind: Simulation of Traveling Convection Vortices. *Geophys. Res. Lett.* 26, 3549–3552. doi:10.1029/1999gl010688
- Tamao, T. (1964a). The Structure of Three-Dimensional Hydromagnetic Waves in a Uniform Cold Plasma. *J. Geomagn. Geoelect.* 16, 89–114. doi:10.5636/jgg.16.89
- Tamao, T. (1964b). Hydromagnetic Interpretation of Geomagnetic SSC. *Rep. Ionos. Space Res. Jpn.* 18, 16–31.
- Tanaka, T., Ebihara, Y., Watanabe, M., Den, M., Fujita, S., Kikuchi, T., et al. (2020). Reproduction of Ground Magnetic Variations during the SC and the Substorm from the Global Simulation and Biot-Savart's Law. *J. Geophys. Res. Space Phys.* 125, e2019JA027172. doi:10.1029/2019ja027172
- Tanaka, T. (2007). Magnetosphere-Ionosphere Convection as a Compound System. *Space Sci. Rev.* 133, 1–72. doi:10.1007/s11214-007-9168-4
- Tsunomura, S. (1998). Characteristics of Geomagnetic Sudden Commencement Observed in Middle and Low Latitudes. *Earth Planet Sp.* 50, 755–772. doi:10.1186/bf03352168
- Tsunomura, S. (1999). Numerical Analysis of Global Ionospheric Current System Including the Effect of Equatorial Enhancement. *Ann. Geophys.* 17, 692–706. doi:10.1007/s00585-999-0692-2
- Tu, J., and Song, P. (2019). On the Momentum Transfer from Polar to Equatorial Ionosphere. *J. Geophys. Res. Space Phys.* 124, 6064–6073. doi:10.1029/2019JA026760
- Vichare, G., Rawat, R., Bhaskar, A., and Pathan, B. M. (2014). Ionospheric Current Contribution to the Main Impulse of a Negative Sudden Impulse. *Earth Planets Space* 66, 92. doi:10.1186/1880-5981-66-92
- Wait, J. R. (1960). On the Theory of the Slow-Tail Portion of Atmospheric Waveforms. *J. Geophys. Res.* 65, 1939–1946. doi:10.1029/jz065i007p01939
- Yumoto, K., Osaki, H., Fukao, K., Shiokawa, K., Tanaka, Y., Solovveyev, S. I., et al. (1994). Correlation of High- and Low-Latitude Pi 2 Magnetic Pulsations Observed at 210° Magnetic Meridian Chain Stations. *J. Geomag. Geoelectr.* 46, 925–935. doi:10.5636/jgg.46.925
- Yumoto, K., Matsuoka, H., Osaki, H., Shiokawa, K., Tanaka, Y., Kitamura, T.-I., et al. (1996). North/south Asymmetry of sc/si magnetic variations observed along the 210 magnetic meridian. *J. Geomag. Geoelectr.* 48, 1333–1340. doi:10.5636/jgg.48.1333

Conflict of Interest: The authors declare that the research was conducted in the absence of any commercial or financial relationships that could be construed as a potential conflict of interest.

Publisher's Note: All claims expressed in this article are solely those of the authors and do not necessarily represent those of their affiliated organizations, or those of the publisher, the editors, and the reviewers. Any product that may be evaluated in this article, or claim that may be made by its manufacturer, is not guaranteed or endorsed by the publisher.

Copyright © 2022 Kikuchi, Araki, Hashimoto, Ebihara, Tanaka, Nishimura, Vichare, Sinha, Chum, Hosokawa, Tomizawa, Tanaka and Kadokura. This is an open-access article distributed under the terms of the Creative Commons Attribution License (CC BY). The use, distribution or reproduction in other forums is permitted, provided the original author(s) and the copyright owner(s) are credited and that the original publication in this journal is cited, in accordance with accepted academic practice. No use, distribution or reproduction is permitted which does not comply with these terms.